molecules

MDPI

Article

^{19}F-NMR Diastereotopic Signals in Two *N*-CHF$_2$ Derivatives of (4*S*,7*R*)-7,8,8-Trimethyl-4,5,6,7-tetrahydro-4,7-methano-2*H*-indazole †

Diana García-Pérez [1], Concepción López [1,*] , Rosa M. Claramunt [1] , Ibon Alkorta [2,*] and José Elguero [2]

[1] Departamento de Química Orgánica y Bio-Orgánica, Facultad de Ciencias, UNED, Senda del Rey 9, E-28040 Madrid, Spain; diana2488@hotmail.com (D.G.-P.); rclaramunt@ccia.uned.es (R.M.C.)

[2] Instituto de Química Médica, CSIC, Juan de la Cierva 3, E-28006 Madrid, Spain; iqmbe17@iqm.csic.es

* Correspondence: clopez@ccia.uned.es (C.L.); ibon@iqm.csic.es (I.A.)

† Dedicated to our friend V. A. Ostrovskii of the St. Petersburg State Institute of Technology, Russia, on the occasion of his 70th birthday.

Abstract: In this paper, we report the anisochrony of the fluorine atoms of a CHF$_2$ group when linked to a pyrazole ring. The pyrazole is part of (4*S*,7*R*)-7,8,8-trimethyl-4,5,6,7-tetrahydro-4,7-methano-2*H*-indazole also known as (4*S*,7*R*)-campho[2,3-*c*]pyrazole, which has two stereogenic centers. Gauge-Independent Atomic Orbital (GIAO)/Becke, 3-parameter, Lee-Yang-Parr (B3LYP)/6-311++G(d,f) calculated ^{19}F chemical shifts of the minimum energy conformations satisfactorily agree with the experimental data. The energy differences between minima need to consider solvent effects (continuum model) to be satisfactorily reproduced.

Keywords: ^{19}F-NMR; diastereotopic; anisochrony; pyrazoles; indazoles; GIAO; B3LYP; PCM

1. Introduction

Anisochrony in NMR is observed when a prochiral group is linked to a molecule possessing a stereogenic center. In these conditions, the studied nuclei became diastereotopic [1–4]. In the majority of cases, the literature reports concern ^{1}H-NMR and often the protons of CH$_2$X groups (e.g., benzyl groups) [5,6]. The phenomenon can be observed on the methyl groups of Me$_2$X substituents (e.g., isopropyl groups), with both ^{1}H- and ^{13}C-NMR [7]. Much less common is the observation of the anisochrony of phenyl substituents in CPh$_2$X groups, also with ^{1}H- and ^{13}C-NMR [8,9].

The observation of diastereotopic signals for other nuclei have been reported less often, but, for instance ^{31}P [10–18] is much more common than for ^{15}N, where only one example has been described [19]. Other seldom-explored nuclei are ^{2}H [20], ^{3}H [21], ^{7}Li [22], and ^{17}O [23].

In the present paper, we present our results concerning the observation of ^{19}F diastereotopic signals. In 1957, anisochronous signals were already observed for F$_2$BrC–C*HBrPh, before the phenomenon was clearly understood [24]. Since then, the phenomenon has been repeatedly described, mainly for CHF$_2$ groups [25–27], but also for CRF$_2$ groups [28,29] as well as CRAr$_2$ (Ar = *meta* and *para* substituted with F atoms) and CR(CH$_2$F)$_2$ [30].

None of the examples reported in the preceding paragraph concern a chiral molecule containing an *N*-CHF$_2$ substituent. There are many examples of azoles bearing a *C*-CHF$_2$ substituent, mainly in agrochemistry [31–33], the field of *N*-CHF$_2$ and *N*-CRF$_2$ azoles is less studied although there are several articles dealing with the structures presented in Figure 1.
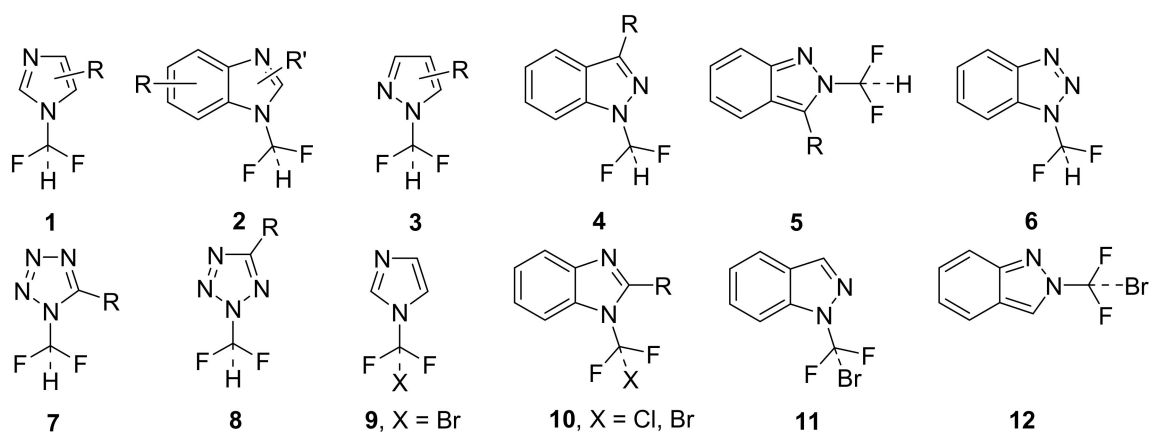
Figure 1. *N*-CHF$_2$, *N*-CClF$_2$, and *N*-CBrF$_2$ azoles and benzazoles.

Imidazoles **1** and benzimidazoles **2** [34–36], pyrazoles **3** [37,38], indazoles **4** and **5** [35,39], benzotriazole **6** [34–36] were reported. Related compounds **9–12** with CXF$_2$ substituents are described in reference [40].

The compounds we have prepared (Scheme 1) and studied, **13** and **14**, are derivatives of (4*S*,7*R*)-7,8,8-trimethyl-4,5,6,7-tetrahydro-4,7-methano-2*H*-indazole also known as (4*S*,7*R*)-campho pyrazole, a compound we have previously investigated [41–44].
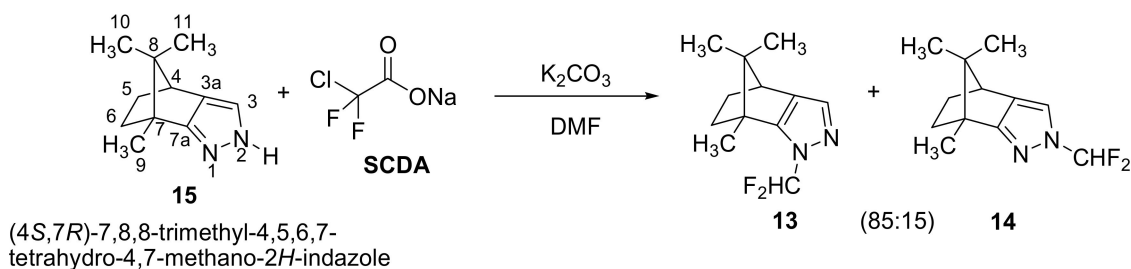
Scheme 1. Synthesis of the *N*-difluoromethyl derivatives **13** and **14** of (4*S*,7*R*)-campho[2,3-*c*]pyrazole. SCDA: sodium chlorodifluoroacetate.

2. Results and Discussion

2.1. Chemistry

As indicated in Scheme 1, compounds **13** and **14** were prepared for the first time by direct difluoromethylation of camphopyrazole **15** with sodium chlorodifluoroacetate (SCDA) [45], according to the Mehta and Greaney conditions [46] or by adding a phase transfer catalyst [47], in both cases using *N,N′*-dimethylformamide as solvent and K$_2$CO$_3$ as base. Both isomers were obtained in an 85:15 ratio (see Experimental Section). The only other paper where the *N*-substitution of **15** was reported (with 1,2-dichloroethane) yielded a 50:50 mixture of both isomers [48]. The structure elucidation of compounds **13** and **14** was based on the close correlation of the ^{13}C chemical shifts of the pyrazole ring with those of a reference compound [48].

2.2. NMR Spectroscopy

In both configurational isomers, the fluorine atoms are diastereotopic, and two distinct signals were observed for each one. From the spectra (Figures 2 and 3 and data given in Supplementary Materials), $^2J(^1\text{H}\text{-}^{19}\text{F})$ and $^2J(^{19}\text{F}\text{-}^{19}\text{F})$ coupling constants can be measured.
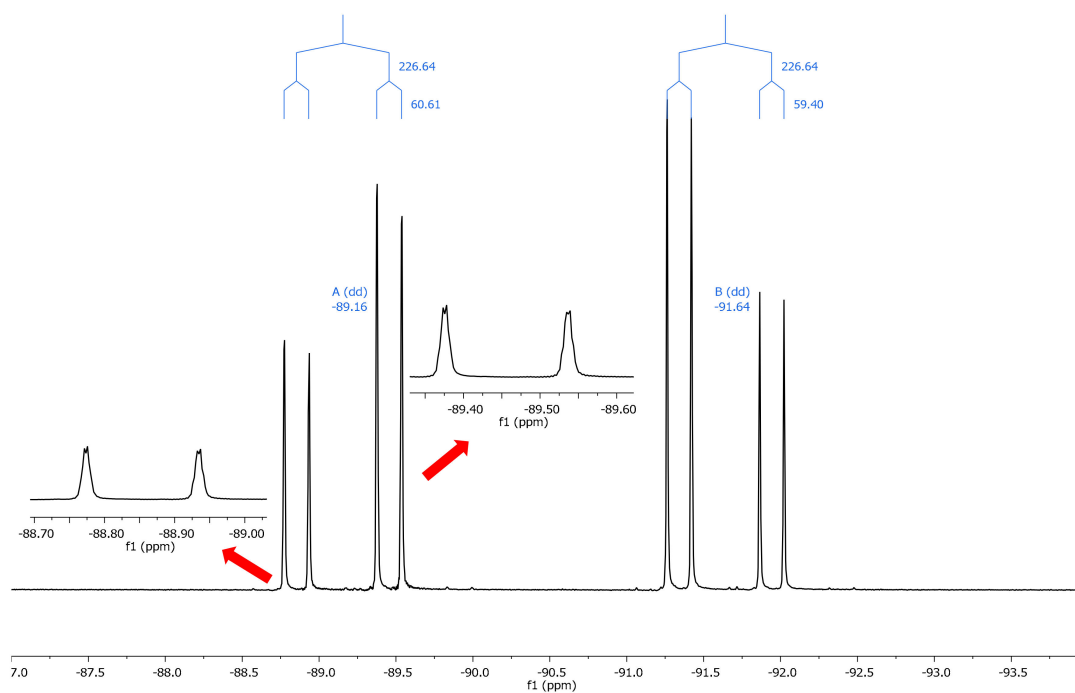
Figure 2. ^{19}F-NMR spectrum of **13** in CDCl$_3$ at 300 K with signals at -89.16 ppm (ddd, $^2J_F = 226.6$, $^2J_H = 60.6$, $^6J_H = 1.4$), and -91.64 (dd, $^2J_F = 226.6$, $^2J_H = 59.4$); the red arrows correspond to the amplification of the left and right side of the signal at -89.16 ppm.
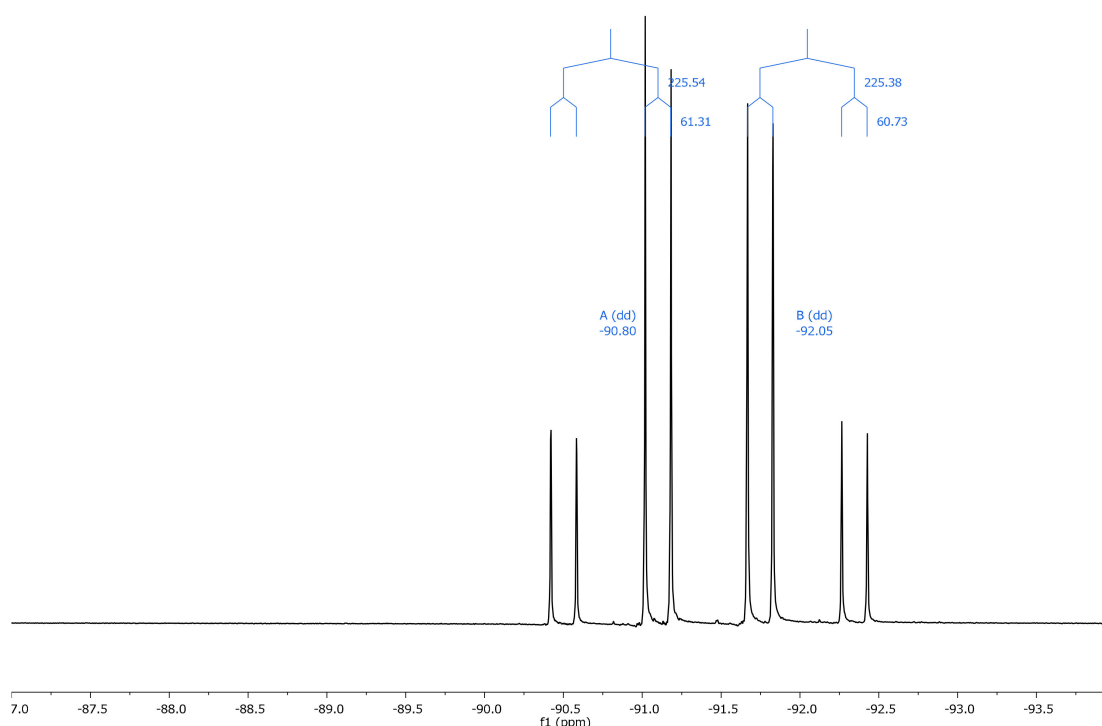
Figure 3. ^{19}F-NMR spectrum of **14** in CDCl$_3$ at 300 K with signals at -90.80 ppm (dd, $^2J_F = 225.5$, $^2J_H = 61.3$), and -92.05 (dd, $^2J_F = 225.4$, $^2J_H = 60.7$).

The $^2J_{FF}$ SSCC (spin-spin coupling constant) in F-C-F compounds is very sensitive to structural aspects, especially the C atom hybridization; for sp^3 carbons range between 3.5 and 340 Hz [49].

There are no $^2J_{FF}$ values published for *N*-azolyl derivatives, and thus the values we have measured (about 225 Hz) are the only representatives of this kind of compound.

In ^{1}H-NMR (see experimental part and Supplementary Material), the most interesting information concerning the CHF$_2$ group where when the anisochrony is larger (compound **13**) the two $^2J_{HF}$ couplings are different and when the anisochrony is smaller (compound **14**) they are identical. Moreover, the signal of the 9-CH$_3$ group in compound **13** shows a long-distance $^6J_{HF}$ coupling of 1.4 Hz (also measured in the ^{19}F-NMR spectrum, see Figure 2); in compound **14**, this coupling is not observed due to the additional bond (it would be a $^7J_{HF}$).

2.3. Computational Results

We have calculated the energy of compounds **13** and **14** as a function of the torsion angle θ about the *N*-(CHF$_2$) bond (defined as H-C-N1-N2, 30-29-7-3 or 30-29-3-7). There are two minima (0 imaginary frequencies)—one near 0° and the other near 180° (Figure 4).

13, θ = 0°　　　　　　　　　　　　　　**13**, θ = 180°
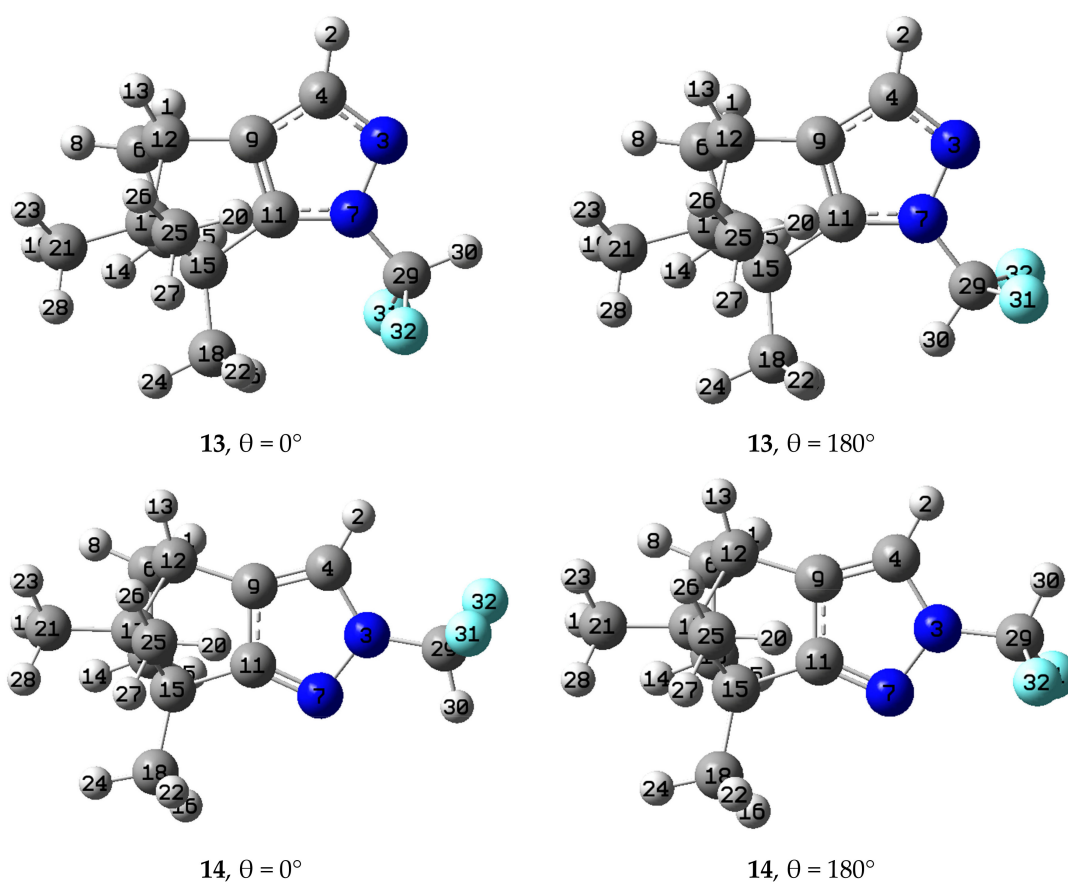
14, θ = 0°　　　　　　　　　　　　　　**14**, θ = 180°

Figure 4. The four minima.

According to the calculations, the 2-substituted isomer **14** is more stable than the 1-substituted isomer **13** by 10.8 kJ·mol^{-1} (both in their minima; i.e., having 0 imaginary frequencies). Note that in camphopyrazole, tautomer 2*H* is more stable than tautomer 1*H* [41,43,44] due to the Mills–Nixon effect [50,51]; once again, tautomerism and isomerism behave similarly.

When the energy was calculated as a function of the torsion angle θ about the *N*-(CHF$_2$) bond, in both cases, the minimum energy conformation corresponds to θ = 0°; i.e., the H atom of the CHF$_2$ group eclipsing the "pyridine-like" N atom of pyrazole, the so-called *syn*-periplanar conformation (Figure 5). The difference between the 0° and the 180° minima are for **13** 15.7 kJ·mol^{-1} and for **14**

11.8 kJ·mol^{-1}, and the transition states are for **13** 23.6 (θ = 104.4°) and 26.6 kJ·mol^{-1} (θ = 255.8°) and for **14** 23.5 (θ = 114.9°) and 23.1 kJ·mol^{-1} (θ = 242.9°).

    This conformational preference can most probably be explained by the dominance of vicinal hyperconjugation, with electron donation from the electron-rich sigma N-N bonding orbital into both of the very electron deficient vicinal C-F anti-bonding orbitals [52–55].

    A natural bond orbital (NBO) analysis shows that the energetic difference between the conformations minima at 0° and 180° can be explained based on the stabilization due to the sum of the charge transfer between the lone pair of the pyridine-like nitrogen and the σ* C-H bond and between the σ N-N and the σ* C-F bonds. This stabilization amount is 6.6 kJ·mol^{-1} in the minima at 0° of **13** and **14**, while in the minima at 180° it is between 1.1 and 1.0 kJ·mol^{-1}, respectively.
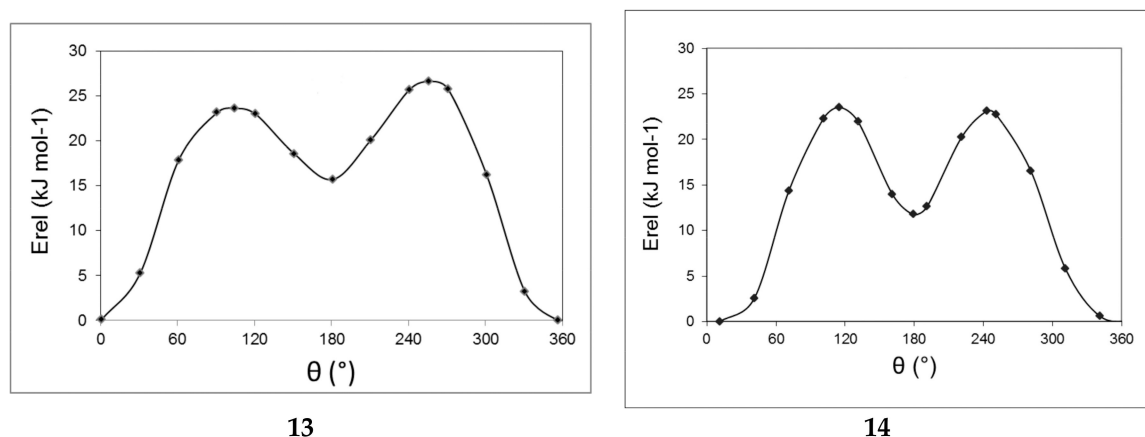

Figure 5. Energy profiles in kJ·mol^{-1} vs. the dihedral angle θ.

    Gauge-Independent Atomic Orbital (GIAO) calculated parameters (absolute shieldings) accounted for the experimental results obtained by multinuclear NMR (^{1}H, ^{13}C, ^{15}N and ^{19}F) (see Supplementary Materials). We will focus on the ^{19}F chemical shifts (Table 1).

Table 1. Calculated (gas phase) and experimental ^{19}F-NMR chemical shifts (CDCl$_3$).

Comp.	θ (°)	^{19}F (31)	^{19}F (32)	$\Delta\delta$ (31–32)	^{19}F (a)	^{19}F (b)	$\Delta\delta$ (a–b) [a]
		Calculated Values			**Experimental Values**		
13	−3.6	−93.18	−89.73	−3.45	−91.64	−89.16	−2.48
13	−179.3	−90.07	−98.52	+8.45			
14	11.1	−92.83	−88.66	−4.17	−92.05	−90.80	−1.25
14	179.3	−85.73	−97.40	+11.67			

[a] The sign is arbitrary because the assignment of **a** and **b** is also arbitrary.

    The four experimental values (−91.6, −89.2, −92.0, −90.8, ppm) are close to the calculated ones for **13** (0°) (−93.2, −89.7 ppm) and for **14** (0°) (−92.8, −88.7 ppm) than for the 180° assignment (−98.5, −90.1, −97.4, −85.7 ppm). Assuming the simplification that only the two minima contribute to the experimental values, a simple interpolation of the type Exp = a × (Calc. abs minima) + (1−a) × (Calc. second minima) lead to **13** = 91.8% of conformer $\theta \approx$ 0° and 8.2% of conformer $\theta \approx$ 180°, and **14** = 81.6% of conformer $\theta \approx$ 0° and 18.4% of conformer $\theta \approx$ 180°. This corresponds at 298.15 K to −6.0 and −3.7 kJ·mol^{-1}, respectively—lower than the calculated differences between both rotamers, but of the same sign. To see if the inclusion of solvent effects improves the agreement, we calculated the differences of energy between minima in CHCl$_3$ (Polarizable continuum model, PCM) obtaining for **13** and **14**, −7.6 and −5.1 kJ·mol^{-1}, respectively—much closer to the experimental results (the TS have

very close values: 19.8 and 19.2 kJ·mol^{-1}); the solvent slightly modifies the geometries, see θ values in Table 2.

We have calculated the chemical shifts in CHCl$_3$, obtaining the values reported in Table 2. With these values, we have calculated that the difference of energies for **13** and **14** are −4.9 and −4.3 kJ·mol^{-1}, respectively, comparable to those obtained for the gas phase (−6.0 and −3.7 kJ·mol^{-1}) to be compared with −7.6 and −5.1 kJ·mol^{-1}.

Table 2. Calculated (CHCl$_3$) and experimental ^{19}F-NMR chemical shifts (CDCl$_3$).

Comp.	θ (°)	^{19}F (31)	^{19}F (32)	Δδ (31–32)	^{19}F (a)	^{19}F (b)	Δδ (a–b) [a]
		Calculated Values			**Experimental Values**		
13	−4.0	−94.07	−90.23	−3.84	−91.64	−89.16	−2.48
13	−179.5	−91.97	−99.34	+7.37			
14	11.2	−94.21	−90.68	−3.53	−92.05	−90.80	−1.25
14	179.4	−86.35	−97.99	+11.64			

[a] The sign is arbitrary because the assignment of **a** and **b** is also arbitrary.

We have also calculated the ^{13}C chemical shifts of the three carbon atoms of the pyrazole ring (C3, C3a, C7a named C4, C9, and C11 in Figure 3). The results are reported in Table 3 and correlates well with the experimental carbon signal shifts, and aided the assignment of the pyrazole ring carbons.

Table 3. Comparison of experimental and calculated ^{13}C chemical shifts.

Comp.	13 exp. CDCl$_3$	13 calc. Gas	13 calc. CHCl$_3$	14 exp. CDCl$_3$	14 calc. Gas	14 calc. CHCl$_3$
C3 (C4)	134.3	133.2	134.4	117.9	117.3	118.2
C3a (C9)	132.1	133.0	133.9	130.2	132.3	133.6
C7a (C11)	153.6	153.7	155.2	169.1	167.5	169.3

3. Experimental Section

3.1. Chemistry

General

All chemicals cited in the synthetic procedure are commercial compounds. Melting points were determined by differential scanning calorimetry (DSC) with a SEIKO DSC 220 C connected to a model SSC5200H disk station. Thermograms (sample size 0.003–0.005 g) were recorded with a scan rate of 5.0 °C. Column chromatography was performed on silica gel 60 (Merck KGaA, Darmstadt, Germany), 70–230 mesh), and elemental analyses using a Perkin-Elmer 240 apparatus (Madrid, Spain).

Preparation of (4*S*,7*R*)-1-(Difluoromethyl)-7,8,8-trimethyl-4,5,6,7-tetrahydro-4,7-methano-1*H*-indazole (**13**) and (4*S*,7*R*)-2-(Difluoromethyl)-7,8,8-trimethyl-4,5,6,7-tetrahydro-4,7-methano-1*H* -indazole (**14**).

Procedure A from Ref. [46]. Into a 100-mL round-bottom three-necked flask equipped with reflux condenser and magnetic stirring, 2 equivalents of sodium chlorodifluoroacetate (SCDA) and 1.5 equivalents of the base (K$_2$CO$_3$) were introduced. The vacuum was established for 15 min and then purged with argon for another 15 min (this process was repeated three times). Six milliliters of *N*,*N*-dimethylformamide (DMF) was added slowly with stirring and under an argon stream, and then 1 equivalent of (4*S*,7*R*)-7,8,8-trimethyl-4,5,6,7-tetrahydro-4,7-methano-2*H*-indazole (**15**) dissolved in 2 mL of DMF was added from an addition funnel over 15 min. The flask was immersed in a silicone bath previously heated to 100 °C and left stirring for 8 h. To control the temperature, a thermometer was used which was connected to the heating plate and immersed in the silicone oil bath. After the reaction time was completed, it was cooled to room temperature and EtOAc (15 mL) and water (15 mL) were added to the mixture. The organic fraction was washed with brine, and the aqueous fraction was extracted with EtOAc. The organic fractions were combined, dried over anhydrous MgSO$_4$, and the

solvent evaporated off. The yield of the reaction crude—in which both isomers are present in a ratio (85% of **13**: 15% of **14**)—is quantitative. The purification was carried out by column chromatography using dichloromethane/hexane (1:1) as eluent. Compound **14** was eluted first.

Procedure B from Ref [47]. Into a 100-mL round-bottom flask equipped with reflux condenser and magnetic stirring, 2 equivalents of SCDA, 3 equivalents of the base (K_2CO_3), 1 equivalent of (4*S*,7*R*)-7,8,8-trimethyl-4,5,6,7-tetrahydro-4,7-methano-2*H*-indazole (**15**), and 0.3 equivalents of tetraethylammonium bromide (TEAB) were dissolved in 10 mL of DMF and the mixture was stirred at 100 °C for 3 h. The resulting mixture was poured into water and extracted with EtOAc, the organic extract containing again an 85:15 mixture of both isomers (overall yield 90%) was treated as previously described in procedure A.

(4S,7R)-1-(Difluoromethyl)-7,8,8-trimethyl-4,5,6,7-tetrahydro-4,7-methano-1H-indazole (**13**). m.p.: 45.4 °C; ^{1}H-NMR: (400.13 MHz, $CDCl_3$) δ = 7.27 (s, H$_3$), 7.14 (dd, ^2J_F = 59.5, ^2J_F = 60.5, CHF$_2$), 2.81 (d, ^3J = 3.8), 2.05 (cm, H$_{5ec}$), 1.03 (cm, H$_{5ax}$), 1.81(cm, H$_{6ec}$), 1.18 (cm, H$_{6ax}$), 1.37 (dd, ^6J_F = 1.4, CH$_3$-9), 0.92 (s, CH$_3$-10), 0.77 (s, CH$_3$-11); ^{13}C-NMR: (100.61 MHz, $CDCl_3$) δ = 153.6 (dd, ^3J_F = 1.6, C7a), 134.3 (dd, ^4J_F = 2.3, C3), 132.1 (C3a), 111.6 (dd, ^1J_F = 246.0, ^1J_F = 248.7, CHF$_2$), 63.2 (C8), 53.7 (C7), 47,6 (C4), 33.0 (C6), 27.4 (C5), 20.1 (CH$_3$-11), 19.5 (CH$_3$-10), 11.6 (dd, ^5J_F = ^5J_F = 1.4, CH$_3$-9); ^{19}F NMR: (376.50 MHz, $CDCl_3$) δ = −89.16 (ddd, ^2J_F = 226.6, ^2J_H = 60.6, ^6J_H = 1.4), −91.64 (dd, ^2J_F = 226.6, ^2J_H = 59.4); ^{15}N-NMR: (40.54 MHz, $CDCl_3$) δ = −177.4 (dd, ^2J_F = ^2J_F = 27.9, N1), −79.9 (N2). Anal. calcd. for $C_{12}H_{16}F_2N_2$: C 63.70, H 7.13, N 12.38. Found: C 63.45, H 7.45, N 12.13.

(4S,7R)-2-(Difluoromethyl)-7,8,8-trimethyl-4,5,6,7-tetrahydro-4,7-methano-1H-indazole (**14**). m.p.: 40.7 °C; ^{1}H-NMR: (400.13 MHz, $CDCl_3$) δ = 7.28 (s, H$_3$), 7.11 (dd, ^2J_F = ^2J_F = 60.9, CHF$_2$), 2.79 (d, ^3J = 4.1), 2.10 (cm, H$_{5ec}$), 1.22 (cm, H$_{5ax}$), 1.88 (cm, H$_{6ec}$), 1.35 (cm, H$_{6ax}$), 1.29 (s, CH$_3$-9), 0.97 (s, CH$_3$-10)), 0.65 (s, CH$_3$-11); ^{13}C-NMR: (100.61 MHz, $CDCl_3$) δ = 169.1 (dd, ^4J_F = ^4J_F = 2.2, C7a), 130.2 (C3a), 117.9 (C3), 111.2 (dd, ^1J_F = 246.4, ^1J_F = 246.5, CHF$_2$), 60.4 (C8), 50.1 (C7), 46.9 (C4), 33.3 (C6), 27.2 (C5), 20.4 (CH$_3$-11), 18.9 (CH$_3$-10), 10.4 (CH$_3$-9); ^{19}F-NMR: (376.50 MHz, $CDCl_3$) δ = −90.80 (dd, ^2J_F = 225.5, ^2J_H = 61.3), −92.05 (dd, ^2J_F = 225.4, ^2J_H = 60.7); ^{15}N-NMR: (40.54 MHz, $CDCl_3$) δ = −177.2 (dd, ^2J_F = ^2J_F = 24.9, N2), N1 not detected. Anal. calcd. for $C_{12}H_{16}F_2N_2$: C 63.70, H 7.13, N 12.38. Found: C 63.37, H 7.48, N 11.98.

3.2. NMR

NMR spectra were recorded on a Bruker (Bruker Biospin GmbH, Rheinstetten, Germany) DRX 400 (9.4 Tesla, 400.13 MHz for ^{1}H, 100.61 MHz for ^{13}C and 40.54 MHz for ^{15}N using a 5-mm inverse-detection H-X probe equipped with a z-gradient coil, at 300 K. Chemical shifts (δ in ppm) are given from internal solvent, $CDCl_3$ 7.26 for ^{1}H and 77.0 for ^{13}C and for ^{15}N, nitromethane (0.00) was used as external reference. Signals were characterized as s (singlet), d (doublet), and cm (complex multiplet) and the *J* coupling constants are given in Hz.

Typical parameters for ^{1}H-NMR spectra were spectral width 4800 Hz and pulse width 9.5 μs at an attenuation level of 0 dB. Typical parameters for ^{13}C-NMR spectra were spectral width 21 kHz, pulse width 12.5 μs, at an attenuation level of −6 dB and relaxation delay 2 s, WALTZ-16 was used for broadband proton decoupling; the Free Induction Decays (FIDs) were multiplied by an exponential weighting (lb = 1 Hz) before Fourier transformation.

Inverse proton detected heteronuclear shift correlation spectra, (^{1}H-^{13}C) gs-HMQC, and (^{1}H-^{13}C) gs-HMBC were acquired and processed using standard Bruker NMR software and in non-phase-sensitive mode. Gradient selection was achieved through a 5% sine truncated shaped pulse gradient of 1 ms.

Selected parameters for (^{1}H-^{13}C) gs-HMQC and (^{1}H-^{13}C) gs-HMBC spectra were spectral width 4800 Hz for ^{1}H and 20.5 kHz for ^{13}C, 1024 × 256 data set, number of scans two (gs-HMQC) or four (gs-HMBC) and relaxation delay 1 s. The FIDs were processed using zero filling in the F_1 domain and a sine-bell window function in both dimensions was applied prior to Fourier transformation. In the

gs-HMQC experiments, Globally Optimized Alternating Phase Rectangular Pulse (GARP) modulation of ^{13}C was used for decoupling. Selected parameters for (^{1}H-^{15}N) gs-HMQC, and (^{1}H-^{15}N) gs-HMBC spectra were spectral width 3500 Hz for ^{1}H and 12.5 kHz for ^{15}N, 1024 × 256 data set, number of scans four, relaxation delay 1 s, 37–60 ms delay for evolution of the ^{15}N-^{1}H long-range coupling. The FIDs were processed using zero filling in the F_1 domain and a sine-bell window function in both dimensions was applied prior to Fourier transformation.

^{19}F-NMR spectra were recorded on the same spectrometer (376.50 for ^{19}F) using a 5 mm Quattro Nucleus Probe (QNP) direct-detection probehead equipped with a z-gradient coil, at 300 K. Chemical shifts (δ in ppm) are given from CFCl$_3$ as external reference (one drop of CFCl$_3$ in CDCl$_3$ (0.00)). Typical parameters for ^{19}F NMR spectra were spectral width of 55 kHz, pulse width of 13.75 µs at attenuation level of −6 dB and relaxation delay of 1 s. WALTZ-16 was used for broadband proton decoupling ^{19}F{^{1}H}, the FIDS were multiplied by an exponential weighting (lb = 1 Hz) before Fourier transformation.

3.3. Computational Details

Calculations were carried out at the B3LYP/6-311++G(d,p) level [56,57]. Subsequent frequency calculations verify that the structures obtained correspond to energetic minima (imaginary frequencies = 0) or to transition states (imaginary frequencies = 1). In the optimization process, the 0° and 180° angles get slightly modified (Tables 1 and 2). These resulting geometries have been used for the calculation of the absolute chemical shieldings with the GIAO method [58,59]. Solvent effects were calculated within the PCM approximation (continuum model) [60–62]. All the calculations have been performed with the Gaussian-09 package [63].

Equations (1)–(4) [64–66] have been used to transform absolute shieldings into chemical shifts:

$$\delta^1\text{H} = 31.0 - 0.97 \times \sigma^1\text{H, (reference TMS, 0.00 ppm)} \tag{1}$$

$$\delta^{13}\text{C} = 175.7 - 0.963 \times \sigma^{13}\text{C, (reference TMS, 0.00 ppm)} \tag{2}$$

$$\delta^{15}\text{N} = -152.0 - 0.946 \times \sigma^{15}\text{N, (reference TMS, 0.00 ppm)} \tag{3}$$

$$\delta^{19}\text{F} = 162.1 - 0.959 \times \sigma^{19}\text{F, (reference CFCl}_3\text{, 0.00 ppm)} \tag{4}$$

The natural bond orbital (NBO) method [67] has been used to obtain the stabilizing charge-transfer interactions in complexes using the NBO-6 program [68].

4. Conclusions

In summary, we have found a new and original example of diastereotopic fluorine atoms, measured two values of $^2J_{\text{FF}}$ in an original environment and successfully carried out GIAO/B3LYP/6-311++G(d,p) calculations of ^{19}F chemical shifts that agree with the calculated energies of the two minima of the potential energy curve when solvent was taken into account.

Author Contributions: J.E. conceived and C.L. designed the experiments; D.G.-P. performed the experiments; C.L. and R.M.C. analyzed the data; I.A. contributed with the computational calculations; R.M.C. and J.E. wrote the paper.

Conflicts of Interest: The authors declare no conflict of interest.

References

1. Devriese, G.; Ottinger, R.; Zimmermann, D.; Reisse, J.; Mislow, K. On the sign of the anisochrony of diastereotopic groups. *Bull. Soc. Chim. Belg.* **1976**, *85*, 167–178. [CrossRef]

2. Nasipuri, D. *Stereochemistry of Organic Compounds. Principles and Applications*, 2nd ed.; New Age International: New Dehli, India, 1994.

3. Eliel, E.L.; Wilen, S.H. *Stereochemistry of Organic Compounds*; John Wiley & Sons: New York, NY, USA, 1994.

4. Alkorta, I.; Elguero, J. Essential versus accidental isochrony of diastereotopic nuclei in NMR spectroscopy. *Struct. Chem.* **2016**, *27*, 671–679. [CrossRef]

5. Elguero, J.; Marzin, C.; Tizané, D. Nuclear Magnetic Resonance of Asymmetrical Nitrogen in a Pentagonal Ring—1,2-Dimethylpyrazolidine. *Tetrahedron Lett.* **1969**, *10*, 513–514. [CrossRef]

6. Elguero, J.; Marzin, C.; Tizané, D. Magnetic Non-equivalence and Nitrogen Inversion in a Series of Dinitrogen Pentagonal Herocycles, 2- and 3-Pyrazolines, Pyrazolidines and Pyrazolidones. *Org. Magn. Reson.* **1969**, *1*, 249–275. [CrossRef]

7. Zvilichovsky, G. The Effect of Solvent on Chemical-shift Non-equivalence of Diastereotopic Geminal Nuclei in (pro)[1]-Chiral *N,N*-Disubstituted 5-Oxo-4-phenyl-2.5-dihydroisoxazol-2-ium-3-olates. *J. Chem. Soc. Perkin Trans.* **1988**, *2*, 2015–2019. [CrossRef]

8. Molina, P.; Alajarín, M.; López-Leonardo, C.; Hernandez Cano, F.; Llamas-Saiz, A.L.; Concepcion Foces-Foces, C.; Rosa Maria Claramunt, R.M.; Elguero, J. 2,4-Bisimino-1,3-diazetidines: Iminophosphoranes, Carbodiimides and Related Betaines. *J. Chem. Soc. Perkin Trans.* **1992**, *1*, 199–210. [CrossRef]

9. Fowler, K.G.; Littlefield, S.L.; Baird, M.C. Synthesis, Structures, and Properties of the Phosphonium-1-indenylide (PHIN) Ligands $1-C_9H_6PPh_3$, $1-C_9H_6PMePh_2$, and $1-C_9H_6PMe_2Ph$ and of the Corresponding Ruthenium(II) Complexes $[Ru(\eta^5-C_5H_5)(\eta^5-PHIN)]PF_6$. *Organometallics* **2011**, *30*, 6098–6107. [CrossRef]

10. Powell, G.L.; Jacobus, J. The Nonequivalence of the Phosphorus Atoms in Cardiolipin. *Biochemistry* **1974**, *13*, 4024–4026. [CrossRef] [PubMed]

11. Pastor, S.D.; Shum, S.P.; Rodebaugh, R.K.; Debellis, A.D.; Clarke, F.H. Sterically Congested Phosphite Ligands: Synthesis, Crystallographic Characterization, and Observation of Unprecedented Eight-Bond ^{31}P, ^{31}P Coupling in the ^{31}P-NMR Spectra. *Helv. Chim. Acta* **1993**, *76*, 900–914. [CrossRef]

12. King, S.A.; DiMichele, L. Multinuclear NMR Observation of a Ru(II)-BINAP Catalyst and Possible Intermediates in the Reduction of Ketoesters. In *Catalysis of Organic Reactions*; Scaros, M.G., Prunier, M.L., Eds.; Marcel Dekker: New York, NY, USA, 1995.

13. Brunel, J.M.; Faure, B. A New ^{31}P NMR Method for the Enantiomeric Excess Determination of Diols and Secondary Diamines with C_2 Symmetry. *Tetrahedron Asymmetry* **1995**, *6*, 2353–2356. [CrossRef]

14. Reich, H.J.; Kulicke, K.J. Dynamics of Solvent Exchange in Organolithium Reagents. Lithium as a Center of Chirality. *J. Am. Chem. Soc.* **1996**, *118*, 273–274. [CrossRef]

15. Yamada, I.; Ohkouchi, M.; Yamaguchi, M.; Yamagishi, T. Asymmetric Hydrogenation of Acrylic Acid Derivatives by Novel Chiral Rhodium-Phosphinediamine Complex Catalysts by Selective Ligation Between Two Amino Units of the Ligand and Electrostatic Interaction. *J. Chem. Soc. Perkin Trans.* **1997**, *1*, 1869–1873. [CrossRef]

16. Bilge, S.; Demiriz, S.; Okumus, A.; Kilic, Z.; Tercan, B.; Kökelek, T.; Buyukgungör, O. Phosphorus-Nitrogen Compounds. Part 13. Syntheses, Crystal Structures, Spectroscopic, Stereogenic, and Anisochronic Properties of Novel Spiro-Ansa-Spiro-, and Spiro-Crypta Phosphazene Derivatives. *Inorg. Chem.* **2006**, *45*, 8755–8767. [CrossRef] [PubMed]

17. Pregosin, P.S. ^{31}P- and ^{13}C-NMR Studies on Metal Complexes of Phosphorus-donors: Recognizing Surprises. *Coord. Chem. Rev.* **2008**, *252*, 2156–2170. [CrossRef]

18. Kruck, M.; Munoz, M.P.; Bishop, H.L.; Frost, C.G.; Chapman, C.J.; Kociok-Köhn, G.; Butts, C.P.; Lloyd-Jones, G.C. BINOL-3,3'-Triflone *N,N*-Dimethyl Phosphoramidites Through-Space ^{19}F, ^{31}P Spin-Spin Coupling with a Remarkable Dependency on Temperature and Solvent Internal Pressure. *Chem. Eur. J.* **2008**, *14*, 7808–7812. [CrossRef] [PubMed]

19. Alkorta, I.; Dardonville, C.; Elguero, J. Observation of Diastereotopic Signals in ^{15}N-NMR Spectroscopy. *Angew. Chem. Int. Ed.* **2015**, *54*, 3997–4000. [CrossRef] [PubMed]

20. Richards, J.C.; Spenser, I.D. ^2H-NMR Spectroscopy as a Probe of the Stereochemistry of Enzymic Reactions at Prochiral Centres. *Tetrahedron* **1983**, *39*, 3549–3568. [CrossRef]

21. Allen, B.D.; Cintrat, J.C.; Faucher, N.; Berthault, P.; Rousseau, B.; O'Leary, D.J. An Isosparteine Derivative for Stereochemical Assignment of Stereogenic (Chiral) Methyl Groups Using Tritium NMR: Theory and Experiment. *J. Am. Chem. Soc.* **2005**, *127*, 412–420. [CrossRef] [PubMed]

22. Salomone, A.; Perna, F.M.; Falcicchio, A.; Nilsson Lill, S.O.; Moliterni, A.; Michel, R.; Florio, S.; Stalke, D.; Capriati, V. Direct Observation of a Lithiated Oxirane: A Synergistic Study Using Spectroscopic, Crystallographic, and Theoretical Methods on the Structure and Stereodynamics of Lithiated *ortho*-Trifluoromethyl Styrene Oxide. *Chem. Sci.* **2014**, *5*, 528–538. [CrossRef]

23. Powers, T.A.; Evans, S.A., Jr. Lanthanide Induced ^{17}O NMR Shifts of Diastereotopic Oxygen Atoms in 1-Thiodecalin 1,1-Dioxide and Related Compounds. *Tetrahedron Lett.* **1990**, *31*, 5835–5838. [CrossRef]

24. Drysdale, J.J.; Phillips, W.D. Restricted Rotation in Substituted Ethanes as Evidenced by Nuclear Magnetic Resonance. *J. Am. Chem. Soc.* **1957**, *79*, 319–322. [CrossRef]

25. Xu, Y.; Tang, P.; Firestone, L.; Zhang, T.T. ^{19}F Nuclear Magnetic Resonance Investigation of Stereoselective Binding of Isoflurane to Bovine Serum Albumin. *Biophys. J.* **1996**, *70*, 532–538. [CrossRef]

26. Vaughan, M.D.; Cleve, P.; Robinson, V.; Duewel, H.S.; Honek, J.F. Difluoromethionine as a Novel ^{19}F-NMR Structural Probe for Internal Amino Acid Packing in Proteins. *J. Am. Chem. Soc.* **1999**, *121*, 8475–8478.

27. Qiu, X.L.; Qing, F.L. Synthesis of *cis*-4-Trifluoromethyl- and *cis*-4-Difluoromethyl-L-pyroglutamic Acids. *J. Org. Chem.* **2003**, *68*, 3614–3617. [CrossRef] [PubMed]

28. Marchione, A.A.; Buck, R.C. Complete Multinuclear Magnetic Resonance Characterization of a Set of Polyfluorinated Acids and Alcohols. *Magn. Reson. Chem.* **2009**, *47*, 194–198. [CrossRef] [PubMed]

29. El Dine, A.N.; Khalaf, A.; Grée, D.; Tasseau, O.; Fares, F.; Jaber, N.; Lesot, P.; Hachem, A.; Grée, R. Synthesis of Enones, Pyrazolines and Pyrrolines with *gem*-Difluoroalkyl Side Chains. *Beilstein J. Org. Chem.* **2013**, *9*, 1943–1948. [CrossRef] [PubMed]

30. Pike, S.J.; De Poli, M.; Zawodny, W.; Raftery, J.; Webb, S.J.; Clayden, J. Diastereotopic Fluorine Substituents as 19F NMR Probes of Screw-sense Preference in Helical Foldamers. *Org. Biomol. Chem.* **2013**, *11*, 3168–3176. [CrossRef] [PubMed]

31. Mykhailiuk, P.K. In Situ Generation of Difluoromethyl Diazomethane for [3 + 2] Cycloadditions with Alkynes. *Angew. Chem. Int. Ed.* **2015**, *54*, 6558–6561. [CrossRef] [PubMed]

32. Du, S.; Tian, Z.; Yang, D.; Li, X.; Li, H.; Jia, C.; Che, C.; Wang, M.; Qin, Z. Synthesis, Antifungal Activity and Structure-Activity Relationships of Novel 3-(Difluoromethyl)-1-methyl-1*H*-pyrazole-4-carboxylic Acid Amides. *Molecules* **2015**, *20*, 8395–8408. [CrossRef] [PubMed]

33. Han, W.Y.; Zhao, J.; Wang, J.S.; Xiang, G.Y.; Zhang, D.L.; Bai, M.; Cui, B.D.; Wan, N.W.; Chen, Y.Z. Diastereoselective [3 + 2] cycloaddition of 3-ylideneoxindoles with in situ generated CF$_2$HCHN$_2$: Syntheses of CF2H-containing spirooxindoles. *Org. Biomol. Chem.* **2017**, *15*, 5571–5578. [CrossRef] [PubMed]

34. Wang, F.; Weizhou, H.; Jinbo, H. Difluoromethylation of *O*-, *S*-, *N*-, *C*-Nucleophiles Using Difluoromethyltri (*n*-butyl)ammonium Chloride as a New Difluorocarbene Source. *Chin. J. Chem.* **2011**, *29*, 2717–2721. [CrossRef]

35. Thomoson, C.S.; Wang, L.; Dolbier, W.R. Use of Fluoroform as a Source of Difluorocarbene in the Synthesis of N-CF$_2$H Heterocycles and Difluoromethoxypyridines. *J. Fluor. Chem.* **2014**, *168*, 34–39. [CrossRef]

36. Prakash, G.K.; Krishnamoorthy, S.; Ganesh, S.K.; Kulkarni, A.; Haiges, R.; Olah, G.A. *N*-Difluoromethylation of Imidazoles and Benzimidazoles Using the Ruppert_Prakash Reagent under Neutral Conditions. *Org. Lett.* **2014**, *16*, 54–57. [CrossRef] [PubMed]

37. Morimoto, K.; Makino, K.; Yamamoto, S.; Sakata, G. Synthesis of Fluoromethyl, Difluoromethyl and Trifluoromethyl Analogues of Pyrazosulfuron-ethyl as Herbicides. *J. Heterocycl. Chem.* **1990**, *27*, 807–810. [CrossRef]

38. Petko, K.I.; Sokolenko, T.M.; Yagulpolskii, L.M. Chemical Properties of Derivatives of *N*-Difluoromethyl- and *N*-2H-Tetrafluoroethylpyrazoles. *Chem. Heterocycl. Comp.* **2006**, *42*, 1177–1184. [CrossRef]

39. Pelc, M.; Huang, W.; Trujillo, J.; Baldus, J.; Turner, S.; Kleine, P.; Yang, S.; Thorarensen, A. An Efficient and Regioselective Difluoromethylation of 3-Iodoindazole with Chlorodifluoromethane. *Synlett* **2010**, 219–222. [CrossRef]

40. Yagupolskii, L.M.; Fedyuk, D.V.; Petko, K.I.; Troitskaya, V.I.; Rudyk, V.I.; Rudyuk, V.V. *N*-Trihalomethyl Derivatives of Benzimidazole, Benzotriazole and Indazole. *J. Fluor. Chem.* **2000**, *106*, 181–187. [CrossRef]

41. Llamas-Saiz, A.; Foces-Foces, C.; Sobrados, I.; Elguero, J.; Meutermans, W. (4*S*,7*R*)-7,8,8-Trimethyl-4,5,6,7-Tetrahydro-4,7-methano-1*H*(2*H*)-indazole (Campho[2,3-*c*]Pyrazole): Comparison Between the X-Ray Structure and Carbon-13 NMR Data in the Solid State. *Acta Crystallogr. Sect. C* **1993**, *49*, 724–729. [CrossRef]

42. Yap, G.P.A.; Claramunt, R.M.; López, C.; García, M.A.; Pérez-Nedina, C.; Alkorta, I.; Elguero, J. The Structures of Chiral and Racemate Campho[2,3-*c*]pyrazole: A Combined Crystallographic, Solid-State NMR and Computational Study. *J. Mol. Struct.* **2010**, *965*, 74–81. [CrossRef]

43. Quesada-Moreno, M.M.; Avilés-Moreno, J.R.; López-González, J.J.; Claramunt, R.M.; López, C.; Alkorta, I.; Elguero, J. Chiral Self-Assembly of Enantiomerically Pure (4*S*,7*R*)-Campho[2,3-*c*]pyrazole in the Solid State: A Vibrational Circular Dichroism (VCD) and Computational Study. *Tetrahedron Asymmetry* **2014**, *25*, 507–515. [CrossRef]

44. Webber, A.L.; Emsley, L.; Claramunt, R.M.; Brown, S.P. NMR Crystallography of Campho[2,3-*c*]pyrazole (Z′=6): Combining High-Resolution ^{1}H-^{13}C Solid-State MAS NMR Spectroscopy and GIPAW Chemical-Shift Calculations. *J. Phys. Chem. A* **2010**, *114*, 10435–10442. [CrossRef] [PubMed]

45. Birchall, J.M.; Cross, G.W.; Haszeldine, R.N. Difluorocarbene. *Proc. Chem. Soc.* **1960**, *81*, 37–96.

46. Mehta, V.P.; Greaney, M.F. S-, N-, and Se-Difluoromethylation Using Sodium Chlorodifluoroacetate. *Org. Lett.* **2013**, *15*, 5036–5039. [CrossRef] [PubMed]

47. Wang, W.; Hua, M.; Huang, Y.; Zhang, Q.; Zhang, X.; Wu, J. Difluoromethylation of 2-Hydroxychalcones Using Sodium 2-Chloro-2,2-difluoroacetate as Difluoromethylating Agent. *Chem. Res. Chin. Univ.* **2015**, *31*, 362–366. [CrossRef]

48. Cabildo, P.; Claramunt, R.M.; Cornago, P.; Lavandera, J.L.; Sanz, D.; Jagerovic, N.; Jimeno, M.L.; Elguero, J.; Gilles, I.; Aubagnac, J.L. Synthesis, structure (NMR and mass spectrometry) and conformational analysis of heterocyclic analogues of dibenzo[*a*,*e*]cycloocta-l,5-diene: 5,6,12,13-tetrahydrobispyrazolo[1,2-a:1′,2′-e][1,2,5,6] tetraazocinediium dihalides. *J. Chem. Soc. Perkin Trans.* **1996**, *2*, 701–711. [CrossRef]

49. Berger, S.; Braun, S.; Kalinowski, H.O. *NMR Spectroscopy of the Non-Elements*; Wiley: New York, NY, USA, 1997; p. 635.

50. Martínez, A.; Jimeno, M.L.; Elguero, J.; Fruchier, A. An Experimental Approach to the Mills-Nixon Effect: Tautomerism of 3(5),4-Polymethylenepyrazoles. *New J. Chem.* **1994**, *18*, 269–277.

51. Alkorta, I.; Elguero, J. Tautomerism and the Mills-Nixon Effect. *Struct. Chem.* **1997**, *8*, 189–195. [CrossRef]

52. Brand, D.J.; Steenkamp, J.A.; Brandt, E.V.; Takeuchi, Y. Conformational studies of (−)-epicatechin-Mosher ester. *Tetrahedron Lett.* **2007**, *48*, 2769–2773. [CrossRef]

53. Brand, D.J.; Steenkamp, J.A.; Omata, K.; Kabuto, K.; Fujiwara, T.; Takeuchi, Y. The Origin of an Unusually Large [19]F Chemical Shift Difference Between the Diastereomeric α-Cyano-α-Fluoro-*p*-Tolylacetic Acid (CFTA) Esters of 3′,4′,5,7-Tetra-*O*-Methylepicatechin. *Chirality* **2008**, *20*, 351–356. [CrossRef] [PubMed]

54. Chen, Z.; Corminboeuf, C.; Mo, Y. Direct Evaluation of the Hyperconjugative Interactions in 1,1,1-Trihalo ethane (CH_3CX_3, X = F, Cl, and Br). *J. Phys. Chem. A* **2014**, *118*, 5743–5747. [CrossRef] [PubMed]

55. Baranac-Stojanovic, M. Theoretical Analysis of the Rotational Barrier in Ethane: Cause and Consequences. *Struct. Chem.* **2015**, *26*, 989–996. [CrossRef]

56. Becke, A.D. Density-Functional Exchange-Energy Approximation with Correct Asymptotic Behavior. *Phys. Rev. A* **1988**, *38*, 3098–3100. [CrossRef]

57. Frisch, M.J.; Pople, J.A. Self-Consistent Molecular Orbital Methods. 25. Supplementary Functions for Gaussian Basis Sets. *J. Chem. Phys.* **1984**, *80*, 3265–3269.

58. Ditchfield, R. Self-consistent Perturbation Theory of Diamagnetism. I. A Gauge-Invariant LCAO (Linear Combination of Atomic Orbitals) Method for NMR Chemical Shifts. *Mol. Phys.* **1974**, *27*, 789–807. [CrossRef]

59. London, F. Quantum Theory of Interatomic Currents in Aromatic Compounds. *J. Phys. Radium.* **1937**, *8*, 397–409. [CrossRef]

60. Miertus, S.; Scrocco, E.; Tomasi, J. Electrostatic interaction of a solute with a continuum. A direct utilization of AB initio molecular potentials for the prevision of solvent effects. *Chem. Phys.* **1981**, *55*, 117–129. [CrossRef]

61. Tomasi, J.; Persico, M. Molecular Interactions in Solution: An Overview of Methods Based on Continuous Distributions of the Solvent. *Chem. Rev.* **1994**, *84*, 2027–2094. [CrossRef]

62. Mennucci, B.; Cammi, R. (Eds.) *Continuum Solvation Models in Chemical Physics. From Theory to Applications*; John Wiley & Sons: Chichester, UK, 2007.

63. Frisch, M.J.; Trucks, G.W.; Schlegel, H.B.; Scuseria, G.E.; Robb, M.A.; Cheeseman, J.R.; Scalmani, G.; Barone, V.; Mennucci, B.; Petersson, G.A.; et al. *Gaussian 09, Revision D.01*; Gaussian, Inc.: Wallingford, CT, USA, 2009.

64. Silva, A.M.S.; Sousa, R.M.S.; Jimeno, M.L.; Blanco, F.; Alkorta, I.; Elguero, J. Experimental measurements and theoretical calculations of the chemical shifts and coupling constants of three azines (benzalazine, acetophenoneazine and cinnamaldazine). *Magn. Reson. Chem.* **2008**, *46*, 859–864. [CrossRef] [PubMed]

65. Blanco, F.; Alkorta, I.; Elguero, J. Statistical analysis of ^{13}C- and ^{15}N-NMR chemical shifts from GIAO/B3LYP/6-311++G** calculated absolute shieldings. *Magn. Reson. Chem.* **2007**, *45*, 797–800. [CrossRef] [PubMed]

66. Fresno, N.; Pérez-Fernández, R.; Jimeno, M.L.; Alkorta, I.; Sánchez-Sanz, G.; Elguero, J.; Del Bene, J.E. Multinuclear NMR Characterization of Cyanuric Fluoride (2,4,6-Trifluoro-1,3,5-triazine). *J. Heterocycl. Chem.* **2012**, *49*, 1257–1259. [CrossRef]

67. Reed, A.E.; Curtiss, L.A.; Weinhold, F. Intermolecular Interactions from a Natural Bond Orbital, Donor–Acceptor Viewpoint. *Chem. Rev.* **1988**, *88*, 899–926. [CrossRef]

68. Glendening, E.D.; Badenhoop, J.K.; Reed, A.E.; Carpenter, J.E.; Bohmann, J.A.; Morales, C.M.; Landis, C.R.; Weinhold, F. *NBO 6.0*; University of Wisconsin: Madison, WI, USA, 2013.

Sample Availability: Samples of the compounds **13**, **14**, **15**, are available from the authors.